Available online at www.sciencedirect.com
SciVerse ScienceDirect
Procedia Engineering 00 (2012) 000–000
Procedia Engineering
www.elsevier.com/locate/procedia

International Symposium on Robotics and Intelligent Sensors 2012 (IRIS 2012)

Modeling and Control Analysis of URRG Monohull Blimp

Herdawatie Abdul Kadir[a,b]*, M. R. Arshad [a], Husaini A.B [a]

[a]*Underwater Robotics Research Group (URRG), School of Electrical and Electronic Engineering ,Engineering Campus, Universiti Sains Malaysia (USM) 14300 Nibong Tebal, Pulau Pinang, Malaysia*
[b]*Department of Robotic & Mechatronic Engineering, Faculty of Electrical and Electronic Engineering, Universiti Tun Hussein Onn Malaysia (UTHM) 86400,Batu pahat,Johor, Malaysia*

Abstract

This paper describes the design of a non rigid airship with the issue of scaling down the size. Nevertheless, the stability and controllability of the airship are significant mainly due to drag and buoyancy forces. These problems can be solved by introducing a proper structure design and reliable control algorithm. In this paper, we proposed an airship design called as “Blimp”. We have described the analysis of motion characteristics without ballonet and the model was characterized based on URRG platform setup. Using the computational fluid dynamic approach (CFD), the aerodynamic coefficients were produced by FLUENT™ package based on geometry meshing using GAMBIT™. The blimp model has been proven to be controllable through implementation of an optimal controller for solving the lateral model navigation issues. Simulation within a range of data reveals that the design achieved the desired motion behavior, thus verified its efficiency and viability.

Keywords: Airship; blimp; modeling; CFD; Optimal Control.

Nomenclature

ν	Lateral velocity perturbation (m/s)
ρ	Roll rate (rad/s)
r	Yaw rate (rad/s)
ϕ	Roll attitude (rad)

1. Introduction

The lighter-than-air vehicles technology started with the Montgolfier brothers when they flied the unmanned hot balloon, took place on June 4, 1783, in Annonay, France. An airship is one of the lighter-than-air vehicle (LTA); establishing different capabilities from airplanes and helicopters. In addition, this vehicles fills the gaps left by the conventional aircraft. Nowadays, airship is commercialized for advertising, ecological monitoring and entertainment product[1]. In general, the conventional types of airship are rigid, semi-rigid and non-rigid. According to [2], a blimp is a non-rigid airship that uses gas with lower densities than air to provide aerodynamics and aerostatics lift. It offers low speed and stationary flying, lower power consumption and environmentally friendly without noise pollution. Furthermore, a blimp is safer without fuel

* Corresponding author. Tel.: +604-5996074; fax: +604-5941023.
E-mail address: watie@uthm.edu.my

requirement and crash landing possibility[3]. These properties make blimp as the best observation platform[4]. In this project, a blimp was used as a platform test bed and no ballonet was considered in this design.

The blimp used helium to generate lift, which had a capacity of 0.064lb/ft^3 (1.02 kg/m^3) lighter than air (1.265 kg/m^3) i.e. 8% lower than hydrogen. This second lightest element is very stable and nonflammable compared to hydrogen which is prone to explosion. Using the aerostatics concept, the blimp buoyancy is defined as:

$$B= V\rho_a \tag{1}$$

Where B is the upward buoyancy force acting on the body which depends on volume V of the body and mean density of the local atmosphere surrounding the body, ρ_a. The blimp utilizes the buoyancy of surrounding air rather than aerodynamics motion unlike other aerial vehicles such as airplane, helicopter and multi rotor drones. This characteristic makes blimp able to stay afloat without expending energy. It also has a propulsion system that enabled it to fly and maneuver. The main blimp structure consists of envelope, gondola, fin and vectored propulsion system. The envelope is the gas bag skin that holds the helium gas and the ellipsoid shape also helps to generate lift and reduce air stream drag. The fins were fixed on the body except for one, which is located at downward, where it is used as a rudder to produce yawing behavior. The gondola is the most important part of the blimp; which is used as holding space for the main controlling unit. It consists of sensors, control board, batteries, and the actuator to help guidance and navigation purposes. It also includes vectored propulsion system for left/right propulsion and controlling the angle of the propeller.

A review on blimp models had been discussed in detail by [5],[6]. A number of non rigid airship models were presented as a rigid body to simplify the modeling process [7],[8],[9],[10]. In this paper, the blimp dynamic was model based on [11] with a few modifications. With recent CFD methods, it is possible to analyze aerodynamic characteristics without the wind-tunnel test data [12].

The purpose of this work was to model the blimp dynamic for lateral control based on aerodynamic coefficient produced by FLUENT™. Due to its small size, the design suffered high instability issues. However, the model proved to be controllable. An optimal controller was proposed to stabilize the yawing movement by controlling the rudder deflection. Analysis on the blimp motion behavior due to rudder deflection was also conducted. The rest of the paper is organized as follows: Section II describes the model by introducing assumption, kinematics and decoupled dynamic model. In Section III, the CFD result is presented. Section IV deals with blimp design evaluation. The control and performances evaluation based on yaw rate, and roll are presented in section V. Finally, Section VI concludes the paper.

2. Mathematical model

This section presents the mathematical model of airship. We are focusing on small size of airship called blimp. The equation of motion (EOM) is based on rigid body dynamic with several assumptions. When developing the airship model, the main difference between conventional fixed-wing craft and airship is the climb parameter. The net buoyancy force for airship in climb is positive. Principally, a blimp is a balloon with a propulsion system. The blimp controls its buoyancy in air similar as underwater vehicles. When a blimp ascends, the thruster will provide upward lift force, and helium makes the vehicle to be positively buoyant and rises up. As it reaches the cruising altitude, thruster angle will create neutral buoyancy. The blimp will able to maneuver, and yawing will be mainly controlled by the rudder. For pitching, it will be controlled through the thruster. To descend, the thruster angle will be set to make it negatively buoyant for landing.

2.1. Basic Assumptions

The overall dynamic model comprises of decoupled longitudinal and lateral states. The EOM is defined based on two frames: earth fixed references frame, Fe and body fixed references frame, F_b. The location of the center of buoyancy, C_b coincides with the center of volume, C_v in the plane of symmetry. The center of gravity is assumed lies below C_b due to its small size and the location of C_g will not change significantly, as illustrated in Fig 1(a). Since blimp is a non rigid body, aeroelastic effects are omitted by assuming the mass remains constant. The motion is described as a perturbation about the initial trimmed flight condition. Finally, the blimp is assumed to have steady low speed rectilinear flight on flat earth with a stationary atmosphere.

The body–fixed frame is a moving coordinate frame, which is fixed to the blimp. The position and orientation are expressed in earth references frame. Fig 1(b). describes the translational *(X,Y,Z)* and rotational velocities *(v,r,q)* in F_b, and position *(x,y,z)* and orientation *(φ,θ,ψ)* illustrate in F_e. According to [11], we have the following equations (2) and (3) that describe the general EOM for airship. The overall EOM will be discussed further through this section.

$$\eta = J(\eta)\nu \tag{2}$$

$$M\dot{v} + fc(v) + fg(\eta) + fd(v) + fp = \tau \tag{3}$$

Detail of this equation will be discussed in next part to study geometrical aspects of motion and forces. The derivation of kinematics and dynamics will be based on F_b and F_e. These frames form right handed orthogonal frame.

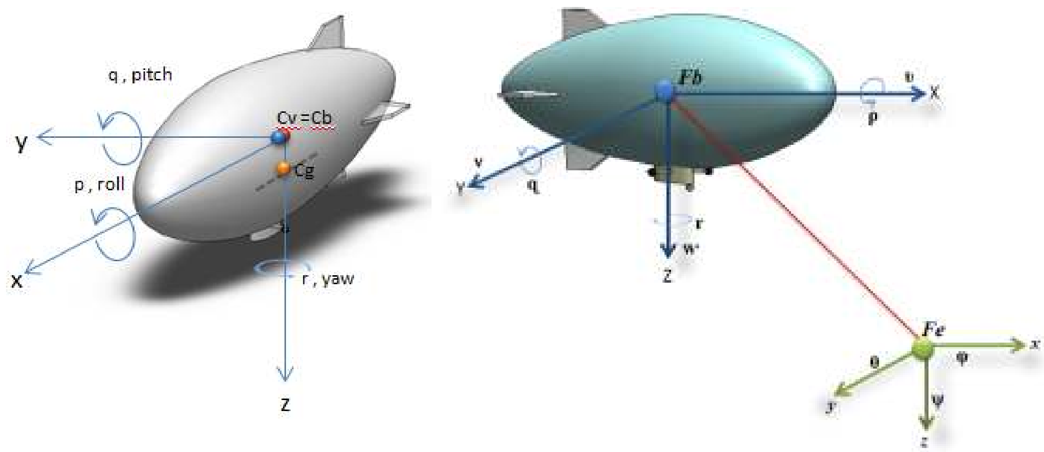

Fig. 1. (a) Motion variables for blimp and (b) Earth References Frame, F_e and Body Fixed Frame, F_b

2.2. Kinematics and dynamic model

A brief introduction on kinematic is given here to help understand the concept. This kinematic model also can be found on underwater and aircraft modeling. According to [13], the relationship between two references frame can be defined as:

$$Fe = R^{Ob}\, Fb \tag{4}$$

The overall 6 DOF Kinematic equations can be derived as:

$$\dot{n} = J(n)v$$

$$\dot{n} = \begin{bmatrix} c\psi c\theta & s\psi c\phi + c\psi s\theta s\phi & s\psi s\phi - c\psi s\theta c\phi & & 0_{3\times3} & \\ -s\psi c\theta & c\psi c\phi - s\psi s\theta s\phi & c\psi s\phi + s\psi s\theta c\phi & & & \\ s\theta & -c\theta s\phi & c\theta c\phi & & & \\ & & & 1 & s\phi t\theta & c\phi t\theta \\ & 0_{3\times3} & & 0 & c\phi & c\psi s\phi + s\psi s\theta c\phi \\ & & & 0 & \dfrac{s\phi}{c\theta} & \dfrac{c\phi}{c\theta} \end{bmatrix} v \tag{5}$$

where $\eta \in R^3 \times S^3$ and $v \in R^6$, $s\theta=\sin(\theta)$ and $c\theta= \cos(\theta)$ valid for $-\pi/2<\theta< \pi/2$. The body fixed angular velocity vector *(p,q,r)* and Euler rate vector $(\phi, \theta, \cup\, \psi)$ are related through a transformation matrix. In this model, the lateral and longitudinal dynamic is taken into account. Fig 4 shows the axes involved in the both decoupled models. The blimp modeling should consider several components such as coriolis effect caused by earth rotation, gravity, buoyancy effect, aerodynamics and the propulsion system. Substituting the (2)-(3) with the element of aerodynamic, gravity, buoyancy, coriolis and propulsion, the full mathematical model of a blimp can be written as follows:

$$\dot{x} = c\psi c\theta\, X + (s\psi c\phi + c\psi s\theta s\phi)Y + (s\psi s\phi - c\psi s\theta c\phi)Z \tag{6}$$

$$\dot{y} = -s\psi c\theta X + (c\psi c\phi - s\psi s\theta s\phi)Y + (c\psi s\phi + s\psi s\theta c\phi)Z \tag{7}$$

$$\dot{z} = s\theta X - c\theta s\phi Y + c\theta c\phi \tag{8}$$

$$\dot{\phi} = p + q\ tan\theta\ sin\phi + rtan\theta cos\phi \tag{9}$$

$$\dot{\theta} = q\ cos\phi - r\ sin\phi \tag{10}$$

$$\dot{\psi} = r\ cos\phi sec\theta + qsin\phi sec\theta \tag{11}$$

$$\dot{u} = 1/m_x\left(X_u u + T_e + X_t\delta_t - (mg - B)(\sin\theta_e + \theta\cos\theta_e) - m_z W_e q - (ma_x - X_{\dot{q}})\dot{q}\right) \tag{12}$$

$$\dot{v} = 1/m_y\left(Y_v v + Y_\delta + (-B)\,\phi\cos\theta_e - m_x U_e r + m_z W_e p + (ma_z + Y_{\dot{p}})\dot{p} - (ma_x - Y\dot{r})\dot{r}\right. \tag{13}$$

$$\dot{w} = 1/m_z(Z_w w + Z_\delta + (mg - B)\ (\cos\theta_e - \ \theta\ sin\ \theta_e) + m_x U_e q + (ma_x - Z\dot{q})\dot{q} \tag{14}$$

3. CFD simulation

The objective of this study is to acquire the aerodynamic coefficient for the blimp model characteristic. In order to perform numerical investigation, geometry meshing was generated using GAMBIT software. The 3D meshing was applied to the air using unstructured triangular mesh, resulting in 52339 cell volumes. Fig 2 shows the flow field computational domain. Then, the mesh file was imported to FLUENT™ for numerical study, steady navier stokes equation was discretized using finite volume and pressure velocity coupling was implemented using simple algorithm. In this work, Kappa-epsilon (k-ε) turbulence models were chosen to investigate the design influence on the aerodynamic behavior. In this case Reynolds's number was 1.7 x10^5 and the flow model was considered as turbulent to cope with the turbulence behavior of Kappa-epsilon(k-ε) turbulence mode as mention in [12].

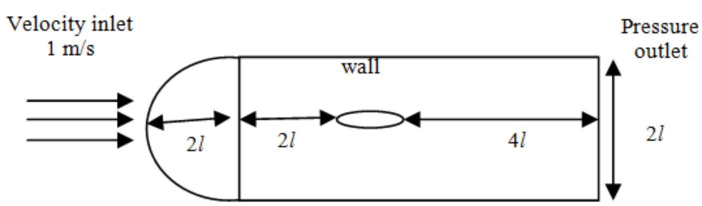

Fig. 2. Geometry drawing for grid generation.

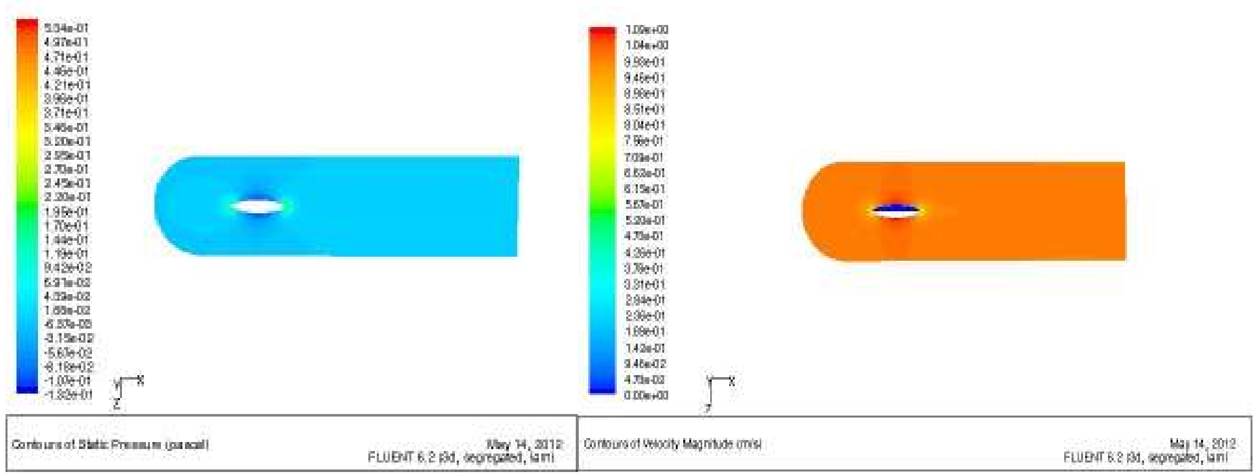

Fig. 3. Blimp contour (a) Pressure contour and (b) Velocity contour.

Fig 3 illustrates the contour generated by the given velocity. The results show the pressure distribution along the body, and forces exert by the body by each point. From the results, we can calculate the drag force, C_d and pressure force along the body. The analysis proved that the C_d, moment coefficient,C_m and lift coefficient,C_L are acceptable however it will be further analyse based on the complete model.

4. Blimp design

This section discusses blimp lateral control using optimal control. The model and control ability were tested using Matlab/Simulink using ode45 solver. This section reveals the geometric and parameter for the blimp were based on the conceptual design using Solidwork software to obtain the value of mass, moment and inertia forces value. Details on blimp specification are presented in Table I. This design was based on the selection for small blimp.

Table 1. Features of the blimp

Items	Specifications
Shape	Ellipsoid
Length , l	1.6764 m
Maximum diameter, d	0.385m
Volume, Vol	19 cu ft
Air density, ρ_a	1.265 kg/m^3
Helium unit lift, L_n	10.359 N/ m^3

Based on the dynamic modeling expressed in Section II, we studied the model performance. In lateral case, the state vector considered for the dynamic characteristics can be represented as follows:

$$x^T = [v \quad p \quad r \quad \phi]$$

$$u^T = [\delta_r]$$

$$a = \begin{bmatrix} Y_v & m_z W_e & -m_x U_e & (mg - B)cos\theta_e \\ 0 & L_p - ma_z W_e & ma_z U_e & -(mga_z - Bb_z)cos\theta_e \\ 0 & ma_x W_e & N_r - Ma_x U_e & (mga_x - Bb_z)cos\theta_e \\ 0 & 1 & 0 & 0 \end{bmatrix} \tag{15}$$

$$b = \begin{bmatrix} 0.5\rho_a \Upsilon \\ 0 \\ 0.5\rho_a \Gamma \\ 0 \end{bmatrix} \tag{16}$$

$$m = \begin{bmatrix} m_y & -ma_z & ma_x & 0 \\ -ma_z & J_x & J_{xz} & 0 \\ ma_x & -J_{xz} & J_z & 0 \\ 0 & 0 & 0 & 1 \end{bmatrix} \tag{17}$$

5. Optimal controller

In this work, the control objective is to maintain the minimum control signal that leads the states towards a target state. By assuming blimp is inhibited by small perturbation about the trimmed equilibrium; it is practical to use decoupled model of blimp[11]. In lateral control design, rudder is used to control yawing. The output affected by this model will be represented by v, p, r and φ states. In order to maneuver, the blimp should have the ability to control position while moving in a trajectory. In LQR design, this method seeks for optimal controller values that minimize control input, u*(t). This design is based on two matrices, Q and R, the state vector and the system input. The linear quadratic controller is given by

$$J(x,u)=\frac{1}{2}x^{t}(t_f)sx(t_f)+\frac{1}{2}\int_{t_0}^{t_f}[x(t)Qx(t)+u^{T}(t)Ru(t)]dt$$

where *S* and *Q* are symmetric, positive-semi definite weighting matrices; and R is a symmetric, positive-definite weighting matrix. The selection of Q and R metric were based on Bryson rules. Based on the model (15) - (17), the LQR gains were given by, K = [0.3754 2.3438 -2.6736 5.8447], respectively. To capture the effect, we introduced impulse signal to verify the control performance. Fig 6 shows that all states successfully regulate to zero as planned.

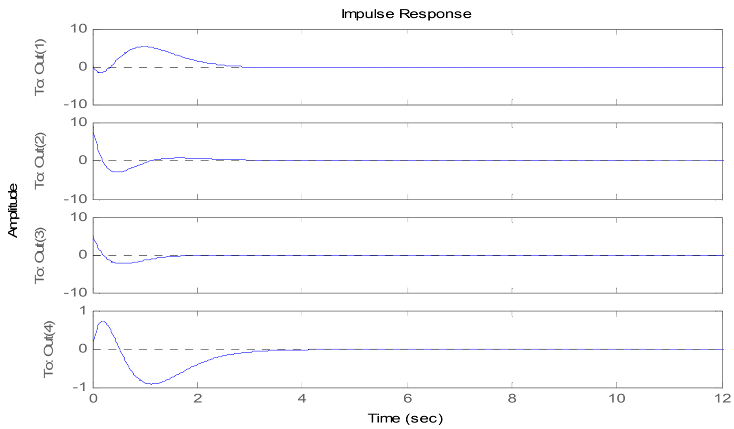

Fig. 4. States output

The gain stresses the model to achieve objective within 5s with acceptable transient responses. Next, we assumed that the vehicle is able to deflect the rudder between +30 to -30 degree. In this case, positive angles contributed to the left deflection. This simulation presented the validation of the states behaviour and error cost.

Positive deflection simulation-The angle of 1 to 30 degrees is the input of the model which is represented by step time of 1 second and initial value of 0 to 60 seconds. The responses of the states were shown in Fig. 7. In this simulation, it showed that by adding angles for yawing, it deflected the body yaw angles and also the roll altitude where each deflection contributed 13 % for yaw rate and 7.4% to the roll angle. Note this based on 180 degrees left and right movement.

Negative deflection simulation- Here the system were excited with an angle of -1 to -30 degree using the same setting in previous simulation. The response was shown in Fig. 8. It can be observed, similar outputs were given with the different signs to represent the left and right directions.

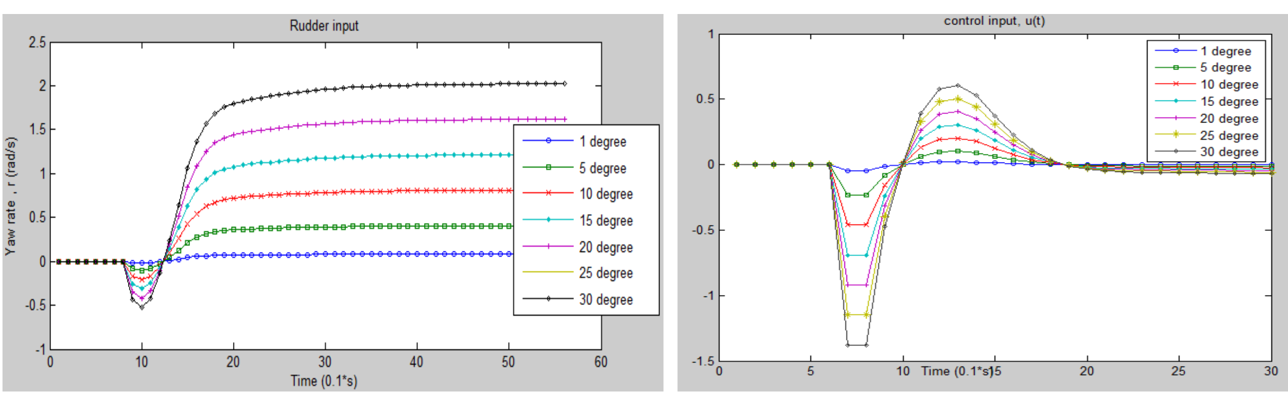

Fig. 7. Positive deflection,δr (a) yaw rates and (b) control signal

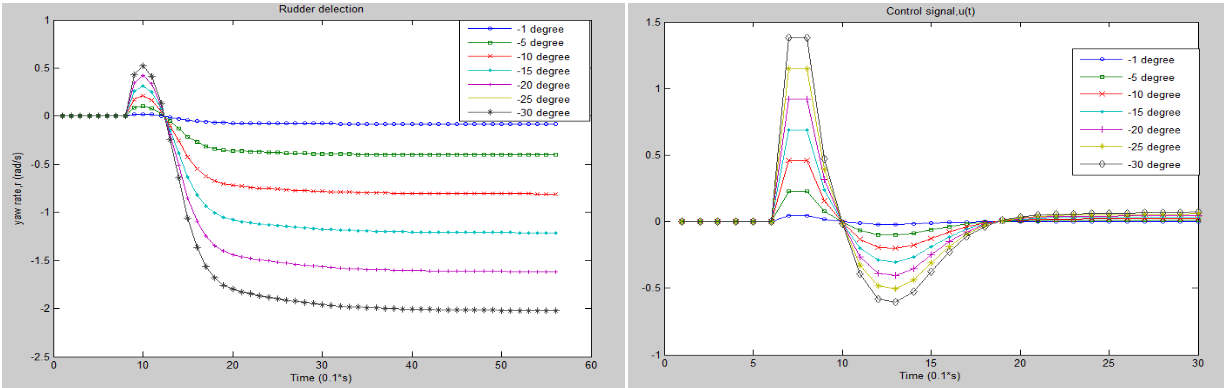

Fig. 8. Negative deflection,δr (a) yaw rates and (b) control signal

The summarize results obtained from the simulation are given in Table II. The input units were described in degree to represent the real behavior of the blimp. It can be observed that, by introducing 1 degree to the rudder contributed approximately r = 4.7^0 /s of body yaw rate. Therefore, the maximum deflection in y-axis gives by r = 141^0 /s corresponded to 73.8% changes within the operating range of 180^0 with settling time of 3.7 s. This behavior was not only effected the yaw rates; it also produced a roll. Here, a small values of p=0.00017^0 /s and ϕ=2.67^0 /s given by $\delta_r = 1^0$. Table III, represents the error percentages for the proposed controller. The average error contributed by the desired input was approximately 6.1% rather small. The highest error was for 10 degree deflection, and the lowest was for 5 degree deflection. Note that the control objective was to minimize the error and control signal between the desired and feedback components. We represented the parameter in modulus form due to almost the same rate given between the positive and negative simulation. Note that δ_r is given in degree.

Table II . States Performances Values

$\delta_{r\,(deg)}$	V,(m/s)	p(deg/s)	r(deg/s)	ϕ(deg)
1	-0.25394	1.77E-04	4.699748	2.668412
5	-1.26971	8.86E-04	23.49874	13.34206
10	-2.53942	1.77E-03	46.99748	26.68412
15	-3.80913	2.66E-03	70.49622	40.02618
20	-5.07884	3.54E-03	93.99497	53.36824
25	-6.34855	4.43E-03	117.4937	66.7103
30	-7.61825	5.32E-03	140.9924	80.05236

Table III . Error percentages

$\lvert\delta_r\rvert$	$\lvert X_r\rvert$	$\lvert y_c\rvert$	$\lvert e_{lqr}\rvert$	$e_{lqr}(\%)$
1	0.046	0.043	0.003	6.0883
5	0.230	0.216	0.014	6.0461
10	0.460	0.432	0.028	6.0883
15	0.690	0.648	0.042	6.0742
20	0.920	0.864	0.056	6.0781
25	1.150	1.080	0.070	6.0870
30	1.380	1.296	0.084	6.0870

The simulation verified the amplitude of control signal is low. This demonstrates the maximum overshoot value of 1.4 and 0.62 undershoot values. The settling time of approximately of 2.5 s for both cases. The results show that in both cases, the blimp was able to achieve controllability and acceptable steady-state response. This means the minimum energy is needed in order to control the blimp position.

Conclusion

This paper presents decoupled lateral model of a small blimp based on aerodynamic coefficient produced by CFD package. The optimal control is used to control the rudder deflection to produce stable yawing rate and roll. We have shown that the design models which include lateral and longitudinal model were unstable but are able to follow the desired performance parameters which enabled us to design the controller. Adjusting certain critical parameters such as blimp mass and volume of the blimp will influence the overall performances of the model.

Acknowledgements

The authors would like to thank Malaysia Ministry of Science, Technology and Innovation (MOSTI), e-Science 305/PELECT/6013410, Ministry of Higher Education (MOHE), Universiti Sains Malaysia and Universiti Tun Hussein Onn Malaysia for supporting the research. They would also like to thank Azian Hariri, Khalid Isa and anonymous reviewers for their comments and suggestions.

References

[1] Yiwei, L., Zengxi,P., Stirling, D., Naghdy, F., 2009. “Control of autonomous airship”, IEEE International Conference on Robotics and Biomimetics (ROBIO), pp. 2457-2462.

[2] González, P., Burgard, W., Sanz, R., Fernández, JL., 2009. “Developing a Low-Cost Autonomous Indoor Blimp”, Journal of Physical Agents 3 p.43-51.

[3] Luca, P., Per, O., Christopher, G., 2011.“Micro- and Nano-Air Vehicles: State of the Art”, International Journal of Aerospace Engineering, Hindawi Publishing Corporation, p.1-17.

[4] Hygounenc, E., Jung, IK., Souères, P., Lacroix, S., 2004.“The autonomous blimp project of laas-cnrs: Achievements in flight control and terrain mapping”. International Journal of Robotics Research, 23 pp. 473-511.

[5] Li, Y., Nahon, M., Sharf, I., 2011. “Airship dynamics modeling: A literature review” , Progress in Aerospace Sciences 47, p.217-239.

[6] Liao, L., Pasternak, I.,2009. “A review of airship structural research and development”, Progress in Aerospace Sciences 45, p. 83-96.

[7] Gomes, SBV., Ramos, JG., 1998. “Airship dynamic modeling for autonomous operation’. IEEE International Conference on Robotics and Automation, pp.3462-3467.

[8] Xiao-liang, W., Ye, M., Xue-xiong, S., 2010. “Modeling of stratosphere airship”, International Symposium on Systems and Control in Aeronautics and Astronautics (ISSCAA) , pp. 738-743.

[9] Bennaceur, S., Abichou, A., Azouz, A., 2008. “ Modeling and control of flexible airship”, AIP Conference Proceeding, pp. 397-407

[10] Gerke, M., Masár, I., 2007. “Modeling, sensorics and control of a robotic airship”. IASTED International Conference on Robotics and Applications, pp. 198-203.

[11] Khoury, GA., Gillet, JD.,1999 . Airship Technology: Cambridge University Press, United Kingdom.

[12] Bessert, N., Frederich, O., 2005. “Nonlinear airship aeroelasticity” , Journal of Fluids and Structures 21(8), p.731-742.

[13] Fossen, TI., 2002. Marine Control Systems: Guidance, Navigation and Control of Ships, Rigs and Underwater Vehicles, Marine Cybernatics: Trondheim, Norway.